Received: 25 June 2021 | Accepted: 21 August 2021

DOI: 10.1002/pamm.202100213

Phase field method for quasi-static brittle fracture: an adaptive algorithm based on the dual variable

Fleurianne Bertrand[1,*]

[1] University of Twente, Drienerlolaan 5, 7522 NB Enschede, Netherlands

An adaptive phase field method for quasi-static brittle fracture is developed. The adaptive refinement of the meshes is based on the error between two stresses: the discontinuous post-processed stresses computed with the displacement approximation and a $H(div)$ conforming dual approximation of the stresses. The algorithm is validated by solving a benchmark problem considering a plate with an edge crack subjected to tension load.

1 Introduction

Fracture propagation is one of the core topics in applied mathematics and engineering. In particular, brittle fracture is an undesirable mode of fracture: it involves crack growth with little deformation of the material around the crack tip and can lead to complete failure of the material very rapidly when a critical load is reached.

Despite the high relevance of the fracture propagation in many challenging applications, the standard finite element method is not accurate enough and only expensive numerical schemes are available to adequately approximate the crack propagation. New classes of highly efficient numerical methods that compute crack propagation with extremely high guaranteed accuracy are therefore essential. In particular, the displacements of an arbitrary cracked body is not likely to be a smooth solution. Therefore the a priori error estimates cannot be achieved using a uniform refinement and the issue of error control is usually tackled via the a posteriori estimates theory and the design of an adaptive strategy (AFEM, see [1]).

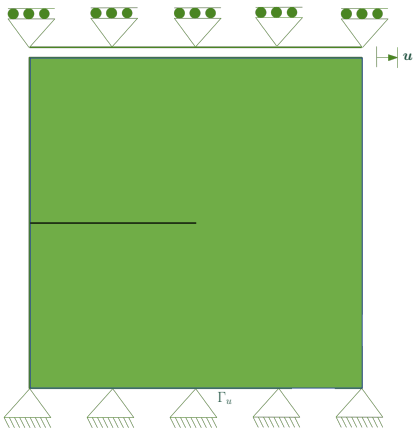

Fig. 1: Geometry of the benchmark test

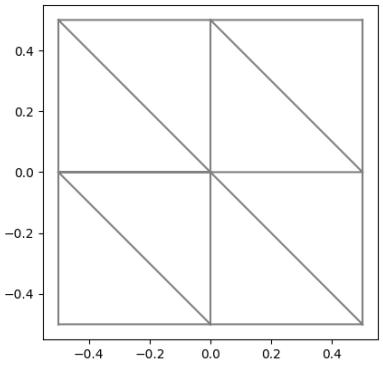

Fig. 2: Initial mesh

Recently, a procedure to implement the staggered phase field model for brittle fracture problems was presented in [2]. The purpose of this paper is to investigate if an adaptive strategy can be developed, such that very accurate simulation results can be obtained with as little computational effort as possible. The error estimator will be based on the dual variable, the stresses. This approach leads to a reconstruction of H(div)-conforming stresses from the displacement approximations in a post-processing step. In fact, accurate flux and stress approximations are of crucial interest in fracture mechanics, although the standard Galerkin approximation usually minimize an energy depending on the primal variable, the displacements. The divergence of those approximation does usually not belong to the Sobolev space H(div), consisting of vector fields for which the components and the weak divergence are square-integrable. A lot of attention has therefore been devoted to the reconstruction of the flux from a primal formulation. The reconstruction procedures for fluxes are also of particular importance for a posteriori error estimation and have a long history with ideas dating back at least as far as [3] (see also [4]). A unified framework for Stokes is presented in [5], polynomial-degree robustness is shown in [6] and extensions to three space dimensions in [7].

In contrast to the case of PDEs involving the full gradient, where equilibrated fluxes can be used, the linear elasticity system involves the symmetric part of the displacement gradient for the definition of the associated stress. This requires the control of the antisymmetric part of the equilibrated stress for the use in an associated a posteriori error estimator.

One possibility is to perform the stress reconstruction in one of the available symmetric H(div)-conforming stress spaces like those introduced by Arnold and Winther [8–10]. However, this complicates the stress reconstruction procedure significantly compared to unsymmetric conforming H(div) elements like the Raviart-Thomas element and motivates equilibrated stress reconstructions with weak symmetry. Weakly equilibrated stress reconstructions were considered for linear elasticity

* Corresponding author: e-mail f.bertrand@utwente.nl

in [11–13]. In particular, a practical algorithm based on the idea of equilibration in broken Raviart-Thomas spaces was presented. In [14], the results were extended to hyperelasticity. The extension to the two-field formulation of the Biot problem involves the reconstruction of the flux of the fluid pressure as well as the reconstruction of total stress tensor and was presented in [15, 16]. In particular, in the tensor reconstruction, the anti-symmetric part was controlled for the use in an associated a posteriori error estimator leading to an a posteriori error bound obtained by a weakly symmetric reconstruction of the total stress tensor combined with a reconstruction of the Darcy velocity.

The paper is organized as follows. The next section reviews the considered model for phase-field method for quasi-static brittle fracture. In section 3, the a posteriori error estimator is derived, together with the conditions for a weakly symmetric stress equilibration. Finally, section 4 shows numerical results and compares uniform and adaptive refinements.

2 Model

Following [2], a linear elastostatic body is considered with a discontinuity occupying the domain $\Omega \subset \mathbb{R}^d$, $d = 2, 3$ and $(\boldsymbol{u}, \phi) : \boldsymbol{\Omega} \to \mathbb{R}^d$ denote the displacement field and the scalar damage variable. The boundary Γ admits the decomposition $\Gamma = \Gamma_D \cup \Gamma_N \cup \Gamma_C$ into three disjoint sets. and essential boundary conditions $(\hat{\boldsymbol{u}}, \hat{\phi})$ are imposed on Γ_D, i.e.

$$\boldsymbol{u} = \hat{\boldsymbol{u}} \text{ on } \Gamma_{\mathrm{D}}, \qquad \phi = \hat{\phi} \text{ on } \Gamma_{\mathrm{D}} \tag{1}$$

Moreover, we impose

$$\left[(1-\phi)^2 + k\right] \nabla \cdot \boldsymbol{\sigma} = \bar{\boldsymbol{t}} \text{ on } \Gamma_{\mathrm{N}} \qquad \nabla\phi \cdot \boldsymbol{n} = 0 \text{ on } \Gamma_{\mathrm{N}} \tag{2}$$

with the outward normal n, the stress tensor $\boldsymbol{\sigma} = \frac{1}{2}\lambda(\mathrm{tr}(\boldsymbol{\varepsilon}))^2 + \mu\,\mathrm{tr}\left(\boldsymbol{\varepsilon}^2\right)$, the symmetric gradient $\varepsilon = \frac{1}{2}\left[\nabla u + \nabla u^{\mathrm{T}}\right]$ and $\boldsymbol{\mu}$ and λ the Lamé constants.

For a given material, we define κ as the product of critical energy release rate and characteristic length while $\bar{\kappa}$ denotes their ratio. When subjected to external tractions $\bar{t}$ on Γ_N, the boundary value problem in the absence of body force reads: find $(\boldsymbol{u}, \phi) : \boldsymbol{\Omega} \to \mathbb{R}^d$ such that

$$\left[(1-\phi)^2 + k\right] \nabla \cdot \boldsymbol{\sigma} = 0 \text{ in } \Omega, \qquad -\kappa\nabla^2\phi + \left[\bar{\kappa} + 2H\right]\phi = 2H \text{ in}$$

under the boundary conditions (1) and (2), where the history variable H is defined as:

$$H = \begin{cases} \psi(\boldsymbol{\varepsilon}), & \psi(\boldsymbol{\varepsilon}) < H_n \\ H_n, & \text{otherwise} \end{cases}$$

Let $\boldsymbol{V} = H^1(\Omega)^d$, $\boldsymbol{V}_0 = H^1_{\Gamma_D}(\Omega)^d$ the subspace of $H^1(\Omega)^d$ where the trace of the functions vanishes on Γ_D and $\boldsymbol{V}_u$ denote the subspace of $H^1(\Omega)^d$ where the essential displacements boundary conditions are satisfied. Similarly, let $\boldsymbol{V}_\phi$ the subspace of $H^1(\Omega)^d$ where the essential damage boundary conditions are satisfied. The weak form of the governing equations is given by: find $(\boldsymbol{u}, \phi) \in \boldsymbol{V}_u \times \boldsymbol{V}_\phi$ such that

$$\int_\Omega \left[(1-\phi)^2 + k\right] \boldsymbol{\sigma}(\boldsymbol{u}) : \boldsymbol{\varepsilon}(\boldsymbol{v})\mathrm{d}\Omega = \int_\Omega \boldsymbol{b} \cdot \boldsymbol{v}\mathrm{d}\Omega + \int_{\Gamma_t} \bar{\boldsymbol{t}} \cdot \boldsymbol{v}\mathrm{d}\Gamma \tag{3}$$

$$\int_\Omega \left(\kappa\nabla\psi\nabla\phi + \psi\left[\bar{\kappa} + 2H\right]\phi\right)\mathrm{d}\Omega = \int_\Omega 2H\psi\mathrm{d}\Omega + \int_\Gamma \nabla\phi \cdot \boldsymbol{n}\psi\mathrm{d}\Gamma \tag{4}$$

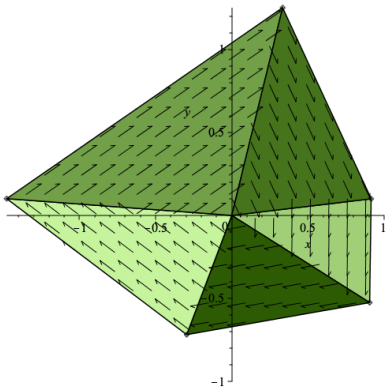

Fig. 3: Divergence free RT_0 function on a non-structured patch

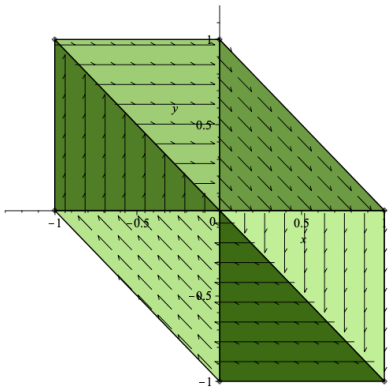

Fig. 4: Divergence free RT_0 function on a structured patch

holds, for all $(\boldsymbol{v}, \psi) \in \boldsymbol{V}_D^2$. We now can consider discrete subspaces consisting of piecewise linear polynomials with respect to a triangulation $\mathcal{T}$. In order to simplify the notation, we denote by $\boldsymbol{V}_\mathcal{T}$ the subspace of $\boldsymbol{V}$ consisting of piecewise linear polynomials with respect to a triangulation $\mathcal{T}$. Our discrete formulation therefore reads: find $(\boldsymbol{u_h}, \phi_h) \in \boldsymbol{V}_{u,\mathcal{T}} \times \boldsymbol{V}_{\phi,\mathcal{T}}$ such that

$$\int_\Omega \left[(1-\phi_h)^2 + k\right] \boldsymbol{\sigma}(\boldsymbol{u}_h) : \boldsymbol{\varepsilon}(\boldsymbol{v}_h) \mathrm{d}\Omega = \int_\Omega \boldsymbol{b} \cdot \boldsymbol{v}_h \mathrm{d}\Omega + \int_{\Gamma_t} \bar{\boldsymbol{t}} \cdot \boldsymbol{v}_h \mathrm{d}\Gamma \tag{5}$$

$$\int_\Omega \left(\kappa \nabla \psi_h \nabla \phi_h + \psi_h \left[\bar{\kappa} + 2H\right] \phi_h\right) \mathrm{d}\Omega = \int_\Omega 2H \psi_h \mathrm{d}\Omega + \int_\Gamma \nabla \phi_h \cdot \boldsymbol{n} \psi_h \mathrm{d}\Gamma \tag{6}$$

holds, for all $(\boldsymbol{v}_h, \psi_h) \in \boldsymbol{V}_{D,\mathcal{T}}^2$.

3 Adaptive Strategy

As in [2], the above variational form is solved using a staggered solver: we first solve for the displacement field using the damage variable. Then, the updated displacement field is used to solve for the damage variable. In a first step, we therefore chose to reconstruct only the displacement variable. For the purpose of the exposition, we restrict ourself to the benchmark problem of the square plate with an edge crack subjected to a displacement at the top in the y direction, as in Figure 1. At a given time iteration, the equation to solve for the displacement is given by

$$\tilde{\kappa}(\nabla \boldsymbol{u}_h, \boldsymbol{\sigma}(\boldsymbol{v}_h)) = 0 \tag{7}$$

This means that we can reconstruct a stress-like variable $\tilde{\boldsymbol{\sigma}}$ with div $\tilde{\boldsymbol{\sigma}} = 0$. Since $\boldsymbol{v}_h$ is a piecewise linear function we reconstruct $\tilde{\boldsymbol{\sigma}}$ in the lowest order Raviart-Thomas space RT_0. Using a partition of unity, we are interested in divergence free functions on a nodal patch, with vanishing flux boundary conditions. The advantage of using the lowest-order Raviart-Thomas space is that, up to a multiplicative function, there is only one (in each dimension) corresponding RT_0 divergence free function $\boldsymbol{\sigma}^B$ on each nodal patch z, namely the curl of a corresponding Lagrange basis function ϕ_z (see Figure 3). We can therefore project $\boldsymbol{\sigma}(\boldsymbol{u}_h \phi_z)$ onto the span $\{\boldsymbol{\sigma}^B\}$ to obtain $\tilde{\boldsymbol{\sigma}}$. The error estimator is then given by $\eta(T) = ||\boldsymbol{\sigma}(\boldsymbol{u}_h \phi_z) - \tilde{\boldsymbol{\sigma}}||_{0,T}$

4 Numerical results

We consider the initial structured triangulation consisting of left triangles presented in Figure 2, and further refinement from this initial mesh. We first refined this mesh 5 times uniformly and compared the results on the second, third, fourth and five triangulation for the time step $\delta t = 10^{-5}$. The effect of the time step is shown in Figure 6 and the effect of the mesh refinement is shown in Figure 5 for the finest time step. Figure 7 shows the crack propagation at successive stages of applied displacements while Figure 8 shows the error estimator. We can see that the adaptive strategy allows for very accurate results with as little computational effort as possible. Future works will extend these results to the higher order case. The behaviour of Raviart-Thomas elements on curved boundaries (see [17–20]) will be crucial to approximate curved crack propagation.

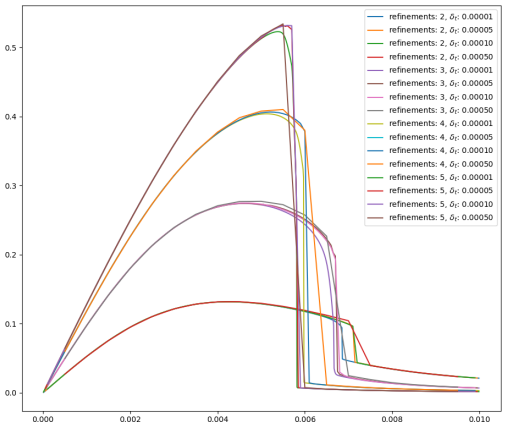

Fig. 5: Effect of the time step and uniform refinements

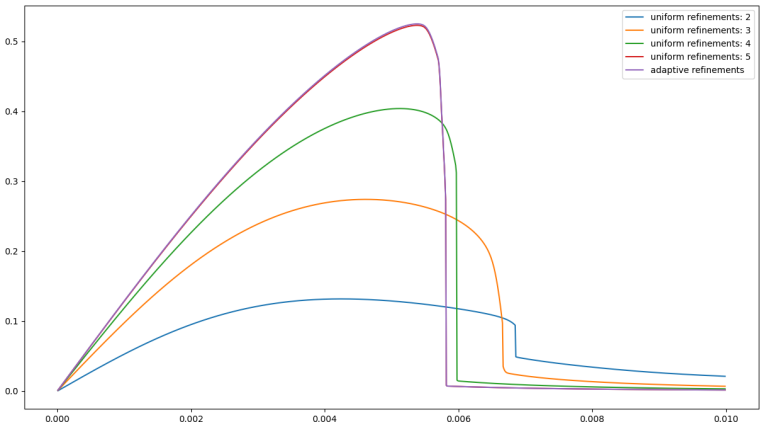

Fig. 6: Comparison of adaptive and uniform refinements

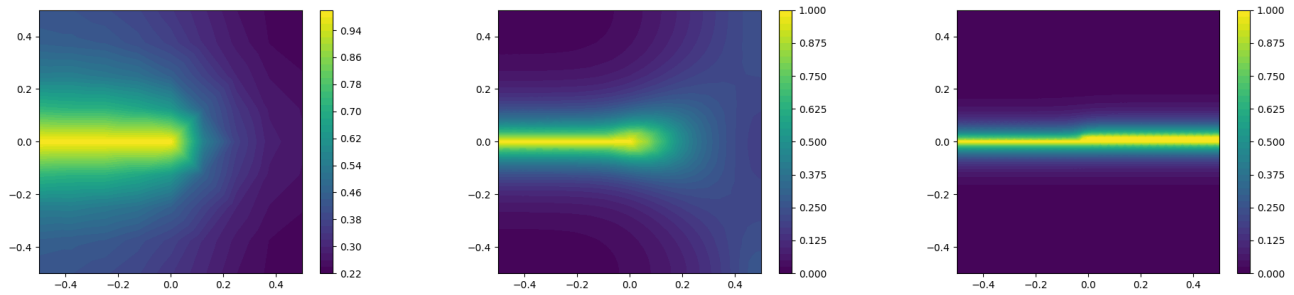

Fig. 7: Error estimator at different time steps

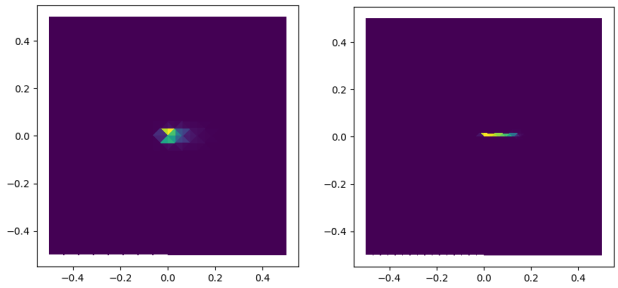

Fig. 8: Damage variable at time steps $t = 0.0057$ and $t = 0.006$

Acknowledgements Open access funding enabled and organized by Projekt DEAL.

References

[1] C. Carstensen, M. Feischl, M. Page, and D. Praetorius, *Axioms of adaptivity*, Comput. Math. Appl. **67**(6), 1195–1253 (2014).
[2] Hirshikesh, S. Natarajan, and R. Annabattula, *A FEniCS implementation of the phase field method for quasi-static brittle fracture*, Frontiers of Structural and Civil Engineering **13**(2), 380–396 (2019).
[3] W. Prager and J. L. Synge, *Approximations in elasticity based on the concept of function space*, Quart. Appl. Math. **5**, 241–269 (1947).
[4] F. Bertrand and D. Boffi, *The Prager-Synge theorem in reconstruction based a posteriori error estimation*, 75^{th} Mathematics of Computation, Contemporary Mathematics **volume 754** (2019).
[5] A. Hannukainen, R. Stenberg, and M. Vohralik, *A unified framework for a posteriori error estimation for the Stokes equation*, Numer. Math. **122**, 725–769 (2012).
[6] A. Ern and M. Vohralik, *Polynomial-degree-robust a posteriori error estimates in a unified setting for conforming, nonconforming, discontinuous Galerkin, and mixed discretizations*, SIAM J. Numer. Anal. **53**, 1058–1081 (2015).
[7] Ern A. and M. Vohralik, *Stable broken H1 and H(div) polynomial extensions for polynomial-degree-robust potential and flux reconstruction in three space dimensions.*, Math. Comp. 89, 322 (2020), 551–594.
[8] D. N. Arnold and R. Winther, *Mixed finite elements for elasticity*, Numer. Math. **92**, 401–419 (2002).
[9] D. N. Arnold, G. Awanou, and R. Winther, *Finite elements for symmetric tensors in three dimensions*, Math. Comp. **77**, 1229–1251 (2008).
[10] C. Carstensen, J. Gedicke, and E. J. Park, *Numerical experiments for the Arnold-Winther mixed finite elements for the Stokes problem*, SIAM Journal on Scientific Computing (2012).
[11] F. Bertrand, M. Moldenhauer, and G. Starke, *A Posteriori Error Estimation for Planar Linear Elasticity by Stress Reconstruction*, Computational Methods in Applied Mathematics **19**(3), 663–679 (2019).
[12] F. Bertrand, B. Kober, M. Moldenhauer, and G. Starke, *Weakly symmetric stress equilibration and a posteriori error estimation for linear elasticity*, Numerical Methods for Partial Differential Equations (2021).
[13] F. Bertrand, B. Kober, M. Moldenhauer, and G. Starke, *Equilibrated Stress Reconstruction and a Posteriori Error Estimation for Linear Elasticity*, in: CISM International Centre for Mechanical Sciences, Courses and Lectures, 2020), pp. 69–106.
[14] F. Bertrand, M. Moldenhauer and G. Starke, *Weakly symmetric stress equilibration for hyperelastic material models*, GAMM Mitteilungen (2020).
[15] F. Bertrand, A. Ern, and F. Radu, *Robust and reliable finite element methods in poromechanics*, Computers and Mathematics with Applications **91**, 1–2 (2021).
[16] F. Bertrand and G. Starke, *A posteriori error estimates by weakly symmetric stress reconstruction for the Biot problem*, Computers and Mathematics with Applications **91**, 3–16 (2020).
[17] F. Bertrand, S. Münzenmaier, and G. Starke, *First-order system least squares on curved boundaries: Higher-order Raviart-Thomas elements*, SIAM Journal on Numerical Analysis **52**(6), 3165–3180 (2014).

[18] F. Bertrand, S. Münzenmaier, and G. Starke, *First-order system least squares on curved boundaries: Lowest-order Raviart-Thomas elements*, SIAM Journal on Numerical Analysis **52**(2), 880–894 (2014).
[19] F. Bertrand and G. Starke, *Parametric Raviart-Thomas elements for mixed methods on domains with curved surfaces*, SIAM Journal on Numerical Analysis **54**(6), 3648–3667 (2016).
[20] F. Bertrand, *First-order system least-squares for interface problems*, SIAM Journal on Numerical Analysis **56**(3), 1711–1730 (2018).

